USING LSM TO INVESTIGATE MALEATED POLYPROPYLENE IN POLYPROPYLENE/GLASS BEAD COMPOSITES

Jeff Toke[1], Marcus T. Cicerone[2], John Muzzy[1]
[1]*Georgia Institute of Technology*
[2]*National Institute of Standards and Technology*

Abstract

In polypropylene (PP)/glass fiber composites often maleated PP (mPP) is blended with PP in order to improve the adhesion of the glass to the PP matrix. We discovered that when the mPP and mPP/PP blends are irradiated with 488 nm light and observed at wavelengths longer than 530 nm, small volumes of auto-fluorescence become apparent. These fluorescent volumes did not show up in the homogeneous PP. The fluorescent volumes in the polymer increase in intensity with increasing acid content in the mPP and in the blends. Blend concentrations of 1, 5, 10, and 20 mass percent (mass%) mPP were analyzed to depths of > 150μm in the polymer blends using a Zeiss LSM510 scanning confocal microscope (1.3NA objective). The results of this study are compared to mechanical properties of PP/glass bead composites made with the homogeneous PP and mPP/PP blends.

Introduction

Polypropylene (PP) is non-polar by nature; therefore, compatibility of PP with polar surfaces and components, such as glass beads and fibers, is poor. Because it is also non-reactive, modifying it to increase its compatibility with polar components is difficult., but some progress has been made. In particular, studies on improving compatibility of PP/polyamide (PA) blends [1-6] and adhesion in PP/glass by blending PP with maleated polypropylene (mPP) have been extensive[7-12]. When the mPP is blended with PP it makes the PP blends more compatible with polar components. In both PP/PA blends and in PP/glass composites, the reactivity of the mPP with an amine group is the basis for improvements in compatibility and adhesion. In the PP/PA blends, an *in-situ* reaction of the anhydride and amine in the PA can form a covalent bond linking the two polymers directly[1,3,4]. In PP/glass composites, amines in γ-amino-propyltrimethoxy silane (γ-APS) on the glass surface may react with the anhydride in the PP/mPP blends[11-13]. It has been shown that there is improved adhesion in (mPP/PP blend)/glass composites with γ-APS coated glass composites as compared to those with PP alone[7-12].

For the anhydride in mPP/PP blends to improve the adhesion in PP/glass composites, knowing the distribution of the grafted maleic anhydride (MAH) is an important piece of the puzzle. In the production of mPP, the MAH is grafted to the PP by reactive extrusion with an organic peroxide[13]. It is known that this process reduces the molecular weight of the PP by chain scission. In recent research, there has been debate about how the MAH is grafted to the PP polymer chains[14-17]. In these studies, there is disagreement as to whether the MAH exists as single units or oligomeric units along the backbone of the polymer, or at the chain ends. Furthermore, there is discussion of how much of the measured MAH content in mPP is bound and unbound MAH or oligomeric MAH species.

Understanding the distribution and form of grafted MAH in mPP is critical in understanding the mechanism of adhesion and compatibilization in anhydride modified PP blends. In this report we explore a new approach to interrogate the distribution of MAH in mPPs and the miscibility of mPP in mPP/PP blends, by using laser scanning confocal microscopy (LSM). With this technique, we obtain 3-D images of homogeneous mPPs and mPP/PP injection molded samples. The images are obtained by focusing monochromatic light to a single point on a focal plane within a specimen by focusing and re-collecting light through a series of pinholes and spectral filters. This confocal technique discriminates against signal outside the volume of interest. Using this technique we obtain signal from a focal volume with the largest dimension (axial) being on the order of a wavelength of light.

The focal volume of the light is scanned through a cross section of the sample by means of a pair of mirrors, and single image planes are obtained. Image data is obtained at different depths of the specimen by moving the specimen stage in the axial direction relative to the objective. For a single sample, individual 2-D images of the cross section are recorded at increasing depths through the sample, and

psuedo 3-D images are produced by the projection of these 2-D images into a volume.

In this study, LSM images of homogeneous mPPs and mPP/PP blends are presented and discussed. The results of the LSM studies are compared to adhesion measurements obtained on non coated (NON) and γ-APS coated (APS) glass bead composites using a strength model.

Experimental

We have examined mPPs ranging in anhydride concentration, as measured by FT-*IR*, from 0.3 mass% to ~10 mass%. All of the samples were blended with a 20 melt flow index (MFI, ASTM D1238) polypropylene homopolymer (hPP) with minimal additives. The hPP was a commercial polypropylene obtained from Huntsman with the trade name P4C5Z-027. The dynamic viscosity of the hPP was 3900 Pa-s, when measured at 1 Hz angular frequency and 180°C. All of the viscosity data reported in this paper were recorded at these conditions. The dynamic viscosity of the mPPs ranged from 0.3 Pa-s to 5100 Pa-s. All of the mPPs were blended and tested at 5 mass% mPP with 95 mass% hPP, with three of the mPPs tested at concentrations ranging from 0 to 100 mass%. A comparison sample was made by blending 2 mass% MAH with the hPP by the same methods described for preparing the mPP/hPP blends. Also, glass bead composites with 25 volume percent beads using the NON and APS beads were made for all the blends with concentrations less than 20 mass% mPP.

The blends and bead composites were fabricated using a 75-ton Sumitomo injection-molding machine. Tensile test specimens as per ASTM D638-00 were molded with a mold temperature of 60°C. All of the blends and bead composites were molded into parts, coarse ground into pellets, and re-molded into final parts for testing. This two-step process was used to insure homogeneous distribution of the beads in the composites and consistency of the blends.

Images of all of the blends and the homogeneous hPP were obtained by LSM from injection-molded specimens, as produced. A 100x (1.3 NA) oil immersion objective was used for all of the images. Laser intensity and detector gain (sensitivity) were also held constant for all samples. 2-D images of cross sectional slices of samples were obtained at increments of 0.67 μm with 488 nm excitation light. Reflectance and fluorescence signals were recorded in tandem with the latter being obtained at wavelengths > 530 nm. We insured the images were not contaminated by reflected light by imaging a gold mirrored surface under conditions that were otherwise identical to those used for sample imaging, and confirming that no signal was detected in the fluorescence channel, even at higher than experimental amplifier gains.

Tensile properties of the bead composites were measured as per ASTM D638-00. The tensile properties were measured on an Instron Model 4466 load frame with a 10 kN load cell with an Instron strain gauge with a 25.4 mm (1 in) guage length and 12.2 mm (0.5 in) travel distance. Five parts were measured and averaged to calculate the average maximum stress for each sample set. The volume percent of glass beads was calculated for each sample using the weight and volume of the specimen.

Results and Discussion

In all of the homogeneous mPPs and the blends of mPP/hPP, small discrete volumes of auto-fluorescence (AF volumes) were observed. The hPP sample showed no signal in the fluorescence channel, even at amplifier gains that were elevated over that used for obtaining the images of the mPPs and blends. Furthermore, the amount of AF volumes increased with increasing MAH content when varying blends of the same mPP were compared.

The images shown in Figure 1 are an example of the increasing AF volume concentration seen as the content of mPP in hPP is increased. The mPP used here had a MAH content of 10 mass%. This particular series of samples is shown as an example because the increase in concentration of AF volumes is most obvious. A similar trend was seen in the 0 to 100 mass% samples of the lower MAH content mPPs. The images shown in Figure 1 are side projections of psuedo-3-D volumes. The decrease in the intensity of AF volumes from the surface to the ~200 μm is due to the limited penetration of light at greater depths. It is observed in both samples that the concentration of AF volumes roughly increases with the concentration of mPP in hPP. Furthermore, the size and distribution of the AF volumes changes as the concentration of mPP in hPP increases.

Figure 2 shows examples of non-blended mPPs with MAH concentration ranging from 1.0 to 2.4 mass%. A relationship between the volume fraction of AF volumes and the concentration of MAH was seen in most of the non-blended mPPs. On the other hand, the 1.2 mass%/197 Pa-s sample deviates from this relationship. Excluding the 1.2 mass%/197 Pa-s sample, the AF volumes increase with increasing MAH concentration, but the size and distribution of the AF volumes are not always the same for a given MAH concentration. This is particularly true for the 1.2 mass%/197 Pa-s sample. We hypothesize that the increase in volume fraction of AF volumes with increasing MAH concentration could be due to

differences in the distribution and/or forms of MAH in this sample. For instance, the fluorescence of singe grafts of MAH evenly distributed throughout the polymer could be greatly different than grafted oligomers of MAH in close vicinity with each other within the polymer. We also note that for the 1.2 mass%/197 Pa-s sample the mass% MAH measured by titration and FT-*IR* were 1.0 and 1.2 mass%, respectively. When compared to the manufacturer's product specifications of 0.4 mass%, the measured values were significantly higher. This was not the case in the other mPPs presented in this paper.

The trends shown in Figure 2 suggest that the AF volumes we observed may give us an indication of the amount and distribution of MAH, but may not show all of the MAH in these samples. The observed AF volumes in these samples may be a function of the form and/or distribution of MAH, as well as the concentration. The differences in comparison of the unblended mPPs show that these images may be an indication of the different distribution and/or forms of MAH in these samples.

Comparisons of the same mPP at different concentration levels in hPP show that the AF volumes increased with increasing mPP concentration (i.e increasing MAH concentration), as the hypothesis would predict. This is an indication that the amount of AF volumes shown using this technique are related to the amount of a particular distribution and/or form of grafted MAH in an particular mPP.

Figure 5 is an image from a control sample, made from 2 mass% MAH blended with hPP. Blending was done in the injection-molding machine, using the same procedure described for making the mPP/hPP blends. The LSM image of this sample was similar to that of the mPPs with ~ 1 to 1.5 mass% MAH, shown in Figure 5.

Figure 3 through 6 show images of non-blended 10 mass%/0.34 Pa-s mPP, non-blended 2.4 mass%/22 Pa-s mPP, and an injection-molded 40 mass% blend of 10 mass%/0.34 Pa-s mPP in hPP respectively. The non-blended samples were made from as-received polymer pellets. We note that LSM images of the as-received pellets were visually the same as the injection-molded samples of the same mPP, indicating that the AF volumes are not caused by injection-molding processing. In each case, the sample was melted on glass slides on a hot plate, covered with a cover slip, then cooled to room temperature and investigated in the same manner as the injection molded samples. Both of the mPP samples had images very similar to the injection-molded plaques with a concentration of AF at the glass/mPP surface of the glass slide, as seen in Figure 3 to Figure 6. Furthermore, when the glass slide was coated with γ-APS the AF signal at the glass slide surface was significantly increased in both mPP samples (data not shown). A sample of hPP was also prepared in this manner, and again, the 3-D projections of the hPP sample showed no AF signal.

The adhesion in the bead composites is measured using the Pukánszky strength model[18]

$$\sigma_c = \left(\frac{1-\phi}{1+2.5\phi} \right) \sigma_m e^{B\phi} \qquad (1)$$

where σ_c is the maximum stress in the bead composite, σ_m is the maximum stress of the unfilled matrix, ϕ is the volume fraction of beads, and B is a constant calculated using experimental data. The B calculated using the above equation is an indication of the strength of adhesion in these composites. As the strength of adhesion in 25 volume percent PP/glass composites reaches a maximum, B increases to an asymptotic value of approximately 3. Variance in B was used to calculate an estimate for the 95% confidence interval in B to be $\pm$ 0.1 .

In previous work[19], the B-value for the hPP with ϕ = 0.25 was 0.32 and 0.45 for the NON and APS beads, respectively. The modified mPP and hPP blends ranged from 0.26 to 2.37 depending on bead type and mPP/hPP blend. In that work, the composites with APS beads had increased adhesion over the NON beads at low concentrations of mPP in hPP, when using mPPs with < 1.0 mass% MAH. However, at higher mPP/hPP concentrations, the NON bead composites showed increased adhesion over the APS bead composites.

The adhesion studies showed a dependence of adhesion improvement on the viscosity and anhydride content. Blends using mPP that was 0.3 mass% MAH/5800 Pa-s showed increasing adhesion up to 20 mass% mPP/hPP, with improved adhesion with APS beads. However, blends using a mPP that was 10 mass% MAH/0.34 Pa-s showed decreased adhesion at > 5 mass% mPP, and reduced adhesion with APS beads. In general, we found that when the viscosity of the mPP was < 200 Pa-s, the adhesion reached a maximum then began to decrease as the mPP/hPP ratio was increased. The fluorescence imaging work presented in this paper suggests that the maximum and subsequent drop off in adhesion strength for low viscosity mPP blends is due to migration of the low viscosity mPP to the surface of the glass beads, decreasing the strength of the interphase in these composites in higher mPP/hPP concentration samples, as is suggested in Figures 4-6.

Conclusions

The LSM images of homogeneous mPPs and mPP/hPP blends showed auto-fluorescence volumes that may be indicative of the MAH distribution in mPP blends. These AF volumes were not evident in any of the unmodified (hPP) LSM images. However, a blend of 2 mass% MAH in hPP did show AF volumes similar to the mPP samples of ~1.0 to 1.5 mass% MAH. In addition, adhesion measurements in low viscosity, higher MAH content mPPs showed a decrease in adhesion with increasing mPP content, after a maximum level was achieved. The decrease of adhesion in these sample could be attributed to the mPPs migrating to the glass surface and weakening the strength of the interphase. LSM images taken of these mPPs on non-coated and γ-APS-coated glass slides showed evidence of the AF volumes in the mPPs migrating to the glass surface. Furthermore, the AF signal was increased at the glass surface in the γ-APS-coated glass slides. More research is required to definitively prove that the AF volumes in these samples is some form of MAH.

References

1. J. Bidaux, G. Smith, N. Bernet, J.E. Manson, *Polymer*, **37** (7),1129 (1996)
2. A. Gonzalez-Montiel, H. Keskkula, D.R. Paul, *J. Polym. Sci. Pol. Phys.*, **33**, 1751 (1995)
3. H. Li, T. Chiba, N. Higashida, Y. Yang, T. Inoue, *Polymer*, **38** (15) 3921 (1997)
4. K. Cho, F., Li, F., *Macromolecules*, **31** 7495 (1998)
5. J. Duvall, C. Sellitti, C. Myers, A. Hiltner, E. Baer, *J. Appl. Polym. Sci.*, **52**, 207 (1994)
6. F. Ide, A. Hasegawa, *J. Appl. Polym. Sci.*, **18**, 963 (1974)
7. M. van den Oever, T. Peijs, *Comps. Part A*, **29A**, 227 (1998)
8. C. Roux, J. DeNault, M.F. Champagne, *J. Appl. Polym. Sci.*, **78**, 2047 (2000)
9. M.J. Folkes, W.K. Wong, *Polymer*, **28**, 1309.
10. X. Zhou, G. Dai, W. Guo, L. Qunfang, *J. Appl. Polym. Sci.*, **76**, 1359 (2000)
11. H. Hamada, K.F. Harada, *Compos. Part A*, **31**, 979 (2000)
12. S. Chou, L. Lin, J. Yeh, *Polym. Polym. Compos.*, **8** (2), 131 (2000)
13. G. Moad, *Prog. Polym. Sci.*, **24**, 81 (1999)
14. B. De Roover, M. Sclavons, V. Carlier, J. Devaux, R. Regras, A. Momtaz, *J. Polym. Sci. Pol. Chem.*, **33**, 829 (1995)
15. B. De Roover, J. Devaux, R. Legras, *J. Polym. Sci. Pol. Chem.*, **34**, 1195 (1996)
16. W. Heinen, C.H. Rosenmöller, C.B. Wenzel, J.M. de Groot, J. Legtenburg, *Macromolecules*, **29**, 1151 (1995)
17. M. Sclavons, V. Carlier, B. DeRoover, P. Franquinet, J. Devaux, R. Legras, *J. Polym. Sci.*, **62** (8), 1205 (1996)
18. B. Pukánszky, *Composites*, **21** (3), 255 (1990)
19. J. M. Toke, *Ph.D. Thesis Dissertation*, Georgia Inst. of Tech., May 2003.

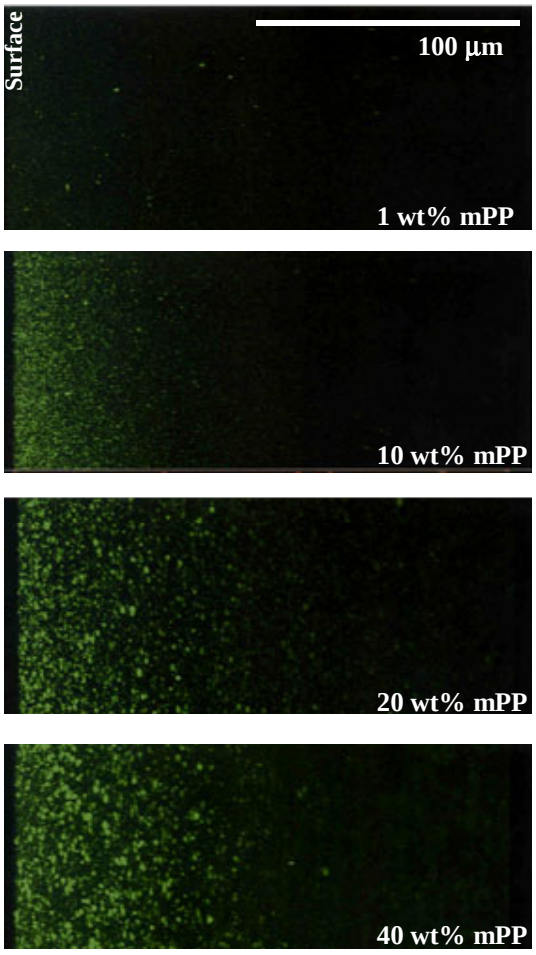

Figure 1: LSM Images of a 10mass% MAH mPP in hPP with increasing mPP/hPP concentration.

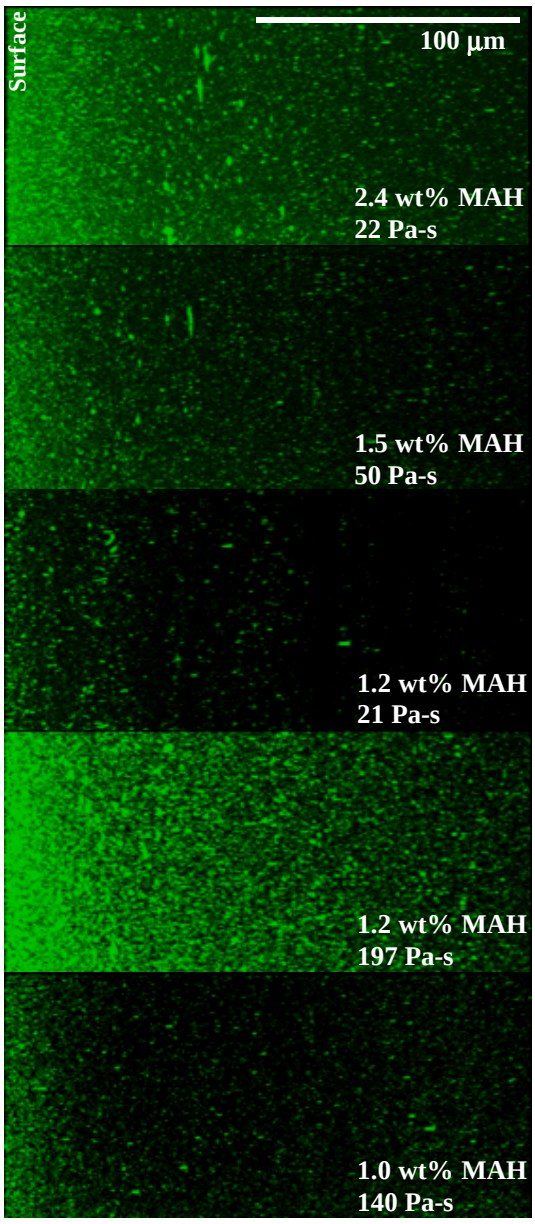

Figure 2: LSM Images of different MAH content homogeneous mPPs.

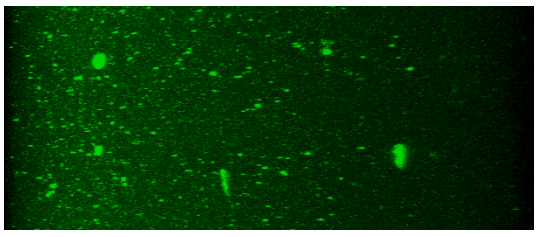

Figure 5: LSM Image of 2 mass% MAH blended with hPP.

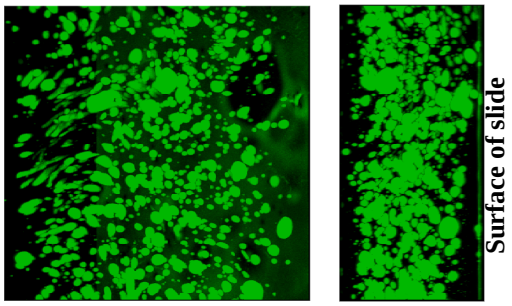

Figure 3: LSM Image of homogeneous ~10mass% MAH/0.34 Pa-s mPP on clean glass slide.

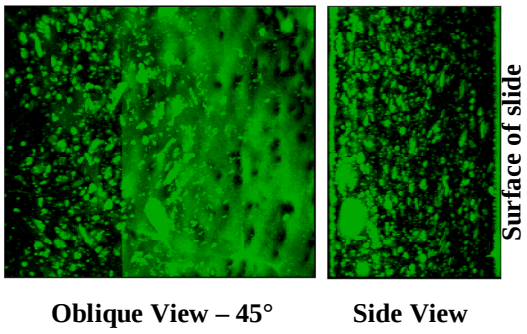

Figure 4: LSM Image of 40 mass% mPP/hPP with ~10mass% MAH/0.34 Pa-s mPP on a clean glass slide.

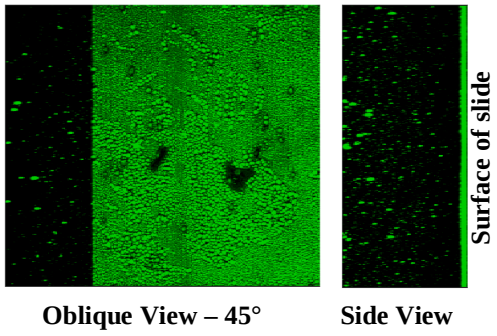

Figure 6: LSM Image of homogeneous 2.4 mass% MAH/22 Pa-s mPP on clean glass slide.